ChemPubSoc Europe

DOI: 10.1002/ejic.201600253

EurJIC European Journal of Inorganic Chemistry

Microreview

Hydrogen Isotope Separation

CLUSTER ISSUE

Quantum Sieving for Separation of Hydrogen Isotopes Using MOFs

Hyunchul Oh*[a] and Michael Hirscher*[b]

Abstract: Hydrogen isotope mixtures can be separated either by confinement in small pores [i.e., "kinetic quantum sieving" (KQS)] or by strong adsorption sites [i.e., "chemical affinity quantum sieving" (CAQS)]. MOFs are excellent candidates for study of these quantum effects, due to their well-defined, tunable pore structures and the potential to introduce strong adsorption sites directly into the framework structure. In this microreview we summarize the recent status of hydrogen isotope separation using MOFs and future strategies relating to it. Furthermore, a state-of-the-art technique for the direct measurement of selectivity with regard to isotope mixtures is introduced. Experimental results relating to separation factors with different pore apertures in the case of KQS and the role of open metal sites in that of CAQS as a function of temperature and gas pressure are given. Furthermore, technologically relevant parameters such as feasible operating pressure and temperature are discussed with respect to possible applications in a temperature swing process.

1. Introduction

In order to solve key challenges facing the world, such as food and energy shortages, climate change, and protection of the environment, new economically and environmentally sustainable energy sources are required.[1] In this regard, nuclear fusion reactors are the promising next generation of large power generators, and they most likely will use hydrogen isotopes as fuel. Therefore, the cost-effective production of deuterium, a stable isotope of hydrogen, appears set to play an indispensable role in the near future.

Moreover, deuterium is not only considered a potential energy source for nuclear fusion reactors, but it is also widely used today in many applications, including as neutron moderators for heavy-water nuclear reactors,[2] for non-radioactive isotopic tracing,[3] in neutron scattering techniques,[4] and others. Despite the demand for it, the mol fraction of natural deuterium is only up to 0.0184 % of all hydrogen on earth (the natural abundance of deuterium in the ocean is approximately 156.25 ppm[5]), and its enrichment from isotope gas mixtures is

[a] *Department of Energy Engineering, Gyeongnam National University of Science and Technology, Jinju, Gyeongnam, 52725, Republic of Korea*
E-mail: oh@gntech.ac.kr
http://h2.gntech.ac.kr
[b] *Max Planck Institute for Intelligent Systems, Heisenbergstr. 3, 70569 Stuttgart, Germany*
E-mail: hirscher@is.mpg.de
http://www.is.mpg.de/schuetz/hydrogen_storage

Hyunchul Oh is an Assistant Professor in the Department of Energy Engineering at Gyeongnam National University of Science and Technology. He obtained his Ph.D. in chemistry from the University of Stuttgart, Germany for his studies at the Max Planck Institute. He worked as a postdoctoral research fellow and associated research fellow at the Max Planck Institute for Intelligent Systems and the Korea Institute of S& T Evaluation and Planning (KISTEP). His current research interests are gas storage and light gas isotope separation using microporous materials.

Michael Hirscher is group leader in "hydrogen storage" at the Max Planck Institute for Intelligent Systems, Stuttgart. He studied physics at the University of Stuttgart, Germany and Oregon State University, Corvallis, USA. For his achievements during his PhD he was awarded the Otto Hahn Medal of the Max Planck Society in 1988. Prior to taking his position in Stuttgart he spent a postdoctoral fellowship at the University of Pennsylvania, Philadelphia, USA. Recently he edited the "Handbook of Hydrogen Storage" and since 2013 has been operating agent of IEA-HIA Task 32 "Hydrogen-based energy storage". His current research interests focus on nanoporous and nanoscale materials for gas storage and separation.

extremely difficult because the two isotopes share almost identical size, shape, and thermodynamic properties. Thus, large-scale industrial separation of hydrogen isotopes is only possible with a limited number of techniques, such as cryogenic distillation or electrolysis of heavy water produced by the Girdler sulfide process, but these techniques tend to be time- and energy-intensive.[6]

In general, gas mixtures can also be separated with the aid of permeable membranes. For classical molecular sieving, the driving force is size difference in mixtures of gases of very different molecular size. The pore size of the membrane is uniform, and only gas molecules smaller than the pore can permeate. This membrane-based gas separation is a very effective and efficient process, and its ease of operation provides a reduction in the process cost of separation. However, in contrast with conventional gas mixture separation, it is not possible to apply these size exclusion methods (molecular sieves) for isotope (e.g., H_2/D_2) separation, due to the hydrogen isotopes' almost identical kinetic diameters, shape, and thermodynamic properties.

Furthermore, isotope separation using porous materials must be based on other mechanisms. Recently, efficient isotope separation by two different mechanisms has indeed been recently reported by several groups.[7] One possible mechanism based on the use of porous materials is kinetic quantum sieving (KQS), a method first proposed by Beenakker et al.[8] They report that if the difference between the entrance pore diameter and the size of the gas molecule become comparable to the de Broglie wavelength, it produces a higher diffusion barrier for lighter isotopes (quantum effect). Owing to this effect, at low temperature molecules of the heavier isotope diffuse more rapidly inside porous materials than lighter molecules, resulting in kinetic quantum isotope molecular sieving. Until now only a few porous materials have been tested experimentally for KQS.[9]

The other mechanism is chemical affinity quantum sieving (CAQS). This can occur when hydrogen isotopes are adsorbed on strongly attracting sites of the host (porous) material. The different molecular masses of the isotopes lead to different adsorption enthalpies (ΔH) of the isotopes, resulting in preferential adsorption of heavier isotopes.

One should note that this quantum effect (and hence differences in adsorption of H_2 and D_2) can be observed in all types of porous materials under certain conditions (e.g., first observed in 1939,[10] in 1962[11] for activated carbons, and in 1988[12] for zeolites). However, very few experimental studies of D_2/H_2 separation in porous adsorbents have been performed so far,[13,14,15,9b,16] and their separation efficiencies were rather low, due to the difficulty of applying conditions maximizing the quantum effects. In order to elucidate (or maximize) these quantum effects, precisely controlled pore size and binding strength is an essential prerequisite. Hence, out of the various porous materials, the new class of porous organic frameworks [e.g., MOFs, covalent organic frameworks (COFs)] are considered to be promising isotope sieving materials because their crystalline frameworks enable precise control (or tuning) of aperture size (e.g., decoration by functional groups at the pore) and functionality (i.e., open metal sites) through accurate design of structures at the molecular level.

As shown in Figure 1, in the field of hydrogen isotope separation the number of publications has been more or less steady over the last five years, whereas reports on hydrogen isotope separation by use of porous materials have been increasing gradually, indicating new developments (Figure 1). Thus, here we describe this new method based on quantum effects and make a comparison with conventional methods. Furthermore, recent progress in experimental studies of hydrogen isotope separation through KQS and CAQS is reviewed, with a particular focus on crystalline – and, therefore, well-defined – porous structures such as metal-organic frameworks or analogous frameworks [e.g., porous coordination polymers (PCPs)]. Finally, the main achievements and issues of hydrogen isotope separation are summarized and future goals are discussed.

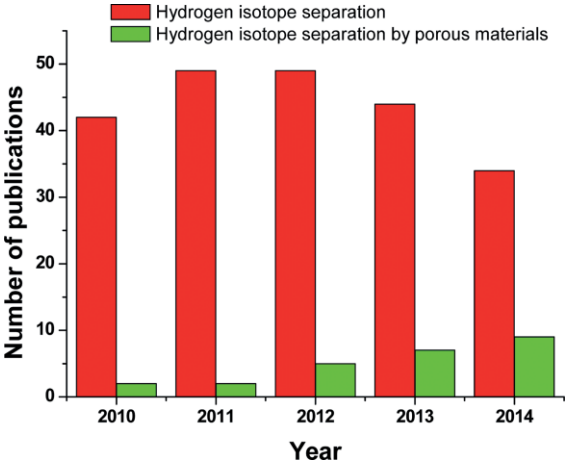

Figure 1. Number of published papers relating to hydrogen isotope separation and to hydrogen isotope separation with the aid of porous materials. Data obtained from Scopus in January 2016.

1.1. General Strategies for H_2/D_2 Separation

Conventional molecular sieves are often utilized in industry for the purification of gas mixtures consisting of components of different molecular size. However, separation of hydrogen isotopes requires special efforts because of their nearly identical size, shape, and thermodynamic properties. Therefore, separation of isotope mixtures is only possible with a limited number of techniques such as cryogenic distillation and the Girdler sulfide (GS) process.

1.1.1. Cryogenic Distillation

Cryogenic distillation has been extensively used in the field of industrial gas separation for many years and is operated at extremely low temperature and high pressure to separate components according to their different boiling temperatures. The basic principle of distillation consists of three steps: (1) generation of a two-phase (vapor/liquid) system by supply of heat, (2) mass transfer between the two coexisting phases (vapor/liquid), and (3) separation of these two vapor/liquid phases. Figure 2 shows a schematic representation of H_2/D_2 separation by cryogenic distillation. One should note that all the other gases (N_2, CO_2, O_2, CH_4, etc.) can be excluded by means either of the "cryogenic

cooling process" or of the "distillation process", due to the huge difference in boiling temperature between hydrogen isotopes and the other gases. This method is advantageous with respect to direct production of liquid D_2 or pure D_2 gas. However, it requires very high energy for the refrigeration and its separation factor is rather low (1.5[6] at 24 K and 3[17] at 20 K), due to the small difference in boiling points (20.3 K and 23.7 K for H_2 and D_2, respectively). Moreover, water vapor has to be removed from the gas mixture before the cryogenic cooling process in order to avoid blockage from freezing in the cryogenic equipment. This may additionally increase the processing costs.

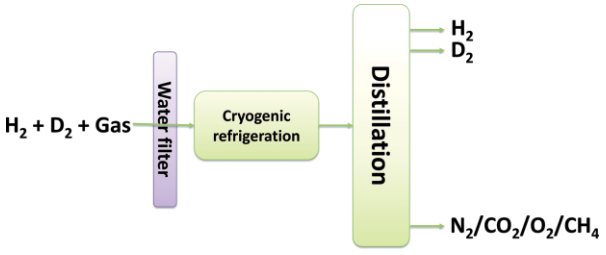

Figure 2. Schematic representation of H_2/D_2 separation by cryogenic distillation.

1.1.2. Chemical Exchange (Girdler Sulfide Process)

The chemical exchange technique makes use of different chemical reaction rates. Although hydrogen and deuterium possess the same number of electrons (and so can be regarded as chemically identical), they undergo chemical reactions at different rates because of the difference in their atomic masses. For that reason, the Girdler sulfide (GS) dual-temperature method is commonly used to produce heavy water in large commercial enrichment plants. This method is an isotopic exchange process between H_2S and ordinary water (containing a small portion of heavy water) that eventually produces D_2O through multiple processing cycles. Figure 3 shows a flow sheet for the GS process. Basically, hydrogen sulfide gas is circulated between a cold and a hot tower. Initially, hydrogen sulfide gas is fed into the cold tower (ca. 303 K) to mix with ordinary water. Then the small portion of heavy water contained in the ordinary water reacts with hydrogen sulfide, producing deuterium sulfide. This product is transferred to a hot tower (ca. 403 K), and reacts with ordinary water, leading to an enrichment of the heavy water content. This cycle is repeated in order to obtain enriched heavy water. Deuterium is then finally produced by electrolysis of the enriched heavy water.

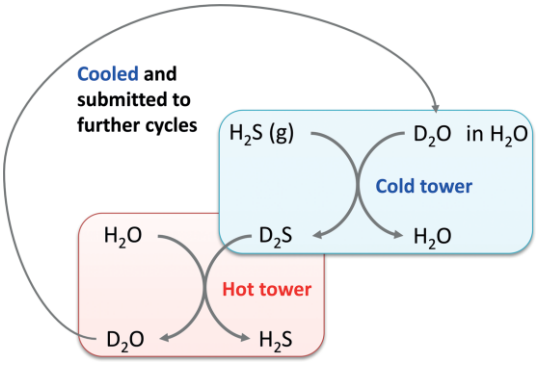

Figure 3. Schematic reaction mechanism for heavy water production by the hydrogen sulfide process.

2. Fundamental Mechanisms of Hydrogen Isotope Separation by Quantum Effects

2.1. Principle of Kinetic Quantum Sieving (KQS)

This concept for isotope separation was first introduced by Beenakker et al. (1995)[8] and is based on the simple model for the adsorption of molecules with hard core diameter in a cylindrical pore with a square well potential. They proposed that isotope separation in nanopores can be possible when the difference between pore size (d) and molecular size (σ) becomes comparable to the de Broglie wavelength of the molecules (λ) when the molecules are restricted in their transverse motion in a given space[8] [Figure 4, a and Equation (1)].

$$\lambda \approx d - \sigma \quad (1)$$

Because D_2 has a shorter λ than H_2, the effective particle size of D_2 is therefore also slightly smaller than for H_2. By exploiting this small difference between H_2 and D_2 with the aid of a sufficiently small opening, a higher mobility of D_2 into the porous medium with small apertures can be observed. This faster diffusion of D_2 than of H_2 leads to isotope separation. A more detailed theoretical explanation follows.

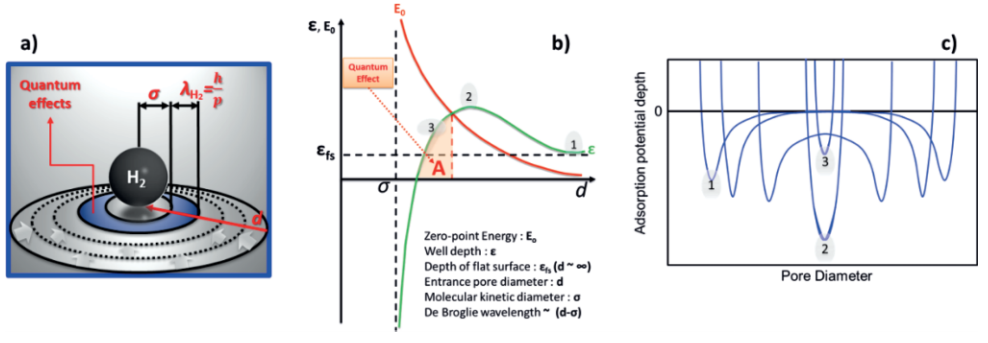

Figure 4. (a) Schematic representation of the quantum confinement effect. (b) Behavior of the well depth (ε) and zero-point energy (E_0) as a function of channel diameter. (c) Adsorption potential depth as a function of pore diameter.

Figure 4 (b) shows the zero-point energy (E_0) of a molecule and the adsorption potential depth (ε) in a narrow pore. As a result of Equation (1), the E_0 of a molecule in a narrow pore is inversely proportional to the de Broglie wavelength [Equation (2)] and the atomic mass (m) of the isotope, meaning that E_0 increases with decreasing d.[8]

$$E_0 \sim \frac{1}{m(d-\sigma)^2} \quad (2)$$

In Figure 4 (b), ε is additionally illustrated as a function of pore diameter (i.e., molecule in a slit channel) starting from its value (ε_{fs}) at a flat surface. The variation of ε with the potential overlap is well demonstrated in Figure 4 (c). For example, when d is large enough, the potentials of the opposite walls do not influence each other and can be approximately regarded as two independent flat surfaces, ε_{fs} (labeled 1 in Figure 4, b–c). This potential overlap gets stronger with decreasing pore width until the potential minima of opposite walls meet each other (labeled 2 in Figure 4, b–c). If d is further reduced, the potential depth starts to decrease (labeled 3 in Figure 4, b–c), and finally when d is the same as or smaller than σ, the molecule can no longer physically penetrate the pore. It is also noted that ε becomes negative before $d = \sigma$ is reached (Figure 4, b), indicating that the electrostatic repulsion of the electron shells between pore and molecule is already occurring for a pore just slightly larger than the molecule, making adsorption difficult.

If equilibrium with the gas in free space is assumed, the density of particles (molecules) inside the channel (pore) per unit length can be estimated as shown below [Equation (3)].[8]

$$n = \underbrace{n_v \frac{\pi}{4}(d-\sigma)^2}_{\text{Free volume per unit length of the channel (pore)}} \underbrace{\sum exp\left(\frac{\varepsilon - E_0}{kT}\right)}_{\text{Boltzmann factor}}, \quad d \geq \sigma \quad (3)$$

where n_v is the gas density outside the channel (pore), k is the Boltzmann constant, and T is absolute temperature.

In region A in Figure 4 (b) (where $d - \sigma$ is close to λ), the zero-point energy (or motion, E_0) of gas molecules overcompensates for the attractive molecule–surface interaction ε (i.e., $E_0/\varepsilon > 1$), resulting in the quantization of the transverse motion of gas molecules in the pore.[8] Hence, according to Equation (3), the molecular density in the channel (pore) will be reduced by a Boltzmann factor $\exp[(\varepsilon - E_0)/kT] < 1$. Because the only difference between isotopes is their mass, the E_0 for lighter isotopes is higher than for heavier ones and hence the density of the lighter isotope in the channel (pore) further decreases in relation to that of the heavier one.

This description proposed by Beenakker[8] can be applied to hydrogen isotope separation by use of microporous materials with pore diameters or apertures similar to the kinetic diameter of the hydrogen isotope under cryogenic conditions. At this nanopore, the hydrogen isotopes each encounter a penetration barrier because $E_0 > \varepsilon$, and this barrier will differ for the isotopes due to the mass (and therefore E_0) difference. Thus, at sufficiently low temperature (at which larger differences exist between the quantized energy levels of H_2 and D_2 adsorbed in a nanopore), the molecular diffusivity of the isotopes will differ[18] inside the porous material, resulting in the separation of the isotopes. That is the so-called kinetic quantum sieving (KQS).

2.2. Principle of Chemical Affinity Quantum Sieving (CAQS)

As an alternative to KQS, it may also be possible to use thermodynamic effects to separate hydrogen isotope mixtures. In general, molecules with the strongest chemical affinity towards the pore surface (or specific adsorption sites) are adsorbed whereas those displaying weaker interaction are not. This holds as long as the pore size is large enough for penetration of both gases, and no diffusion barrier exists inside the porous material.[19] Similarly, isotope molecules may also adsorb on strongly attracting sites of the host material with different affinities because the different molecular masses lead to different zero-point energies (ZPEs) and thus different adsorption enthalpies (ΔH) for each isotope.

In the case of adsorbed molecular hydrogen on the surface, six degrees of freedom – the vibration of the center of the hydrogen molecule towards the adsorption site of the host, the vibration of the intramolecular bond, and two rotational and two translational degrees of freedom – contribute to the ZPE and the partition function, and thus to the enthalpy. Depending on the affinity strength of the adsorption site, the last four degrees might be hindered. The first degree of freedom (vibration of adsorbed H_2 on adsorption sites) is the one that is most strongly influenced by the host material. Hence, a significant difference in their adsorption enthalpies may provide preferential uptake of heavier isotopes, leading to a large separation factor even at liquid nitrogen temperature (77 K) and above.

Figure 5 shows the physisorption potential energy of hydrogen isotopes on a porous material possessing two different adsorption sites, qualitatively describing the ZPEs for hydrogen isotopes [e.g., H_2 (black line) and D_2 (red line)]. The strength of each binding site is represented by the depth of the potential well. It can be seen that the steeper the interaction potential, the larger the difference between the ZPEs of H_2 and of D_2. As already mentioned, the different molecular masses imply different ZPEs, meaning different adsorption enthalpies (ΔH). Consequently, the larger the difference in ΔH, the more

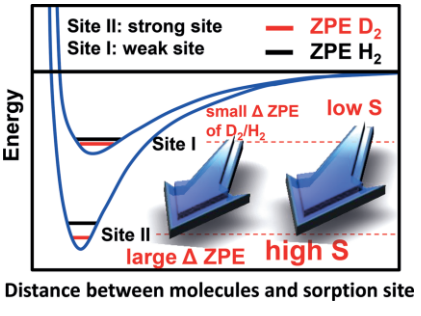

Figure 5. Qualitative plot of the strengths of the adsorption sites. ZPEs are shown qualitatively for H_2 (black) and D_2 (red). The strength of each binding site is demonstrated by the depth of the potential well.

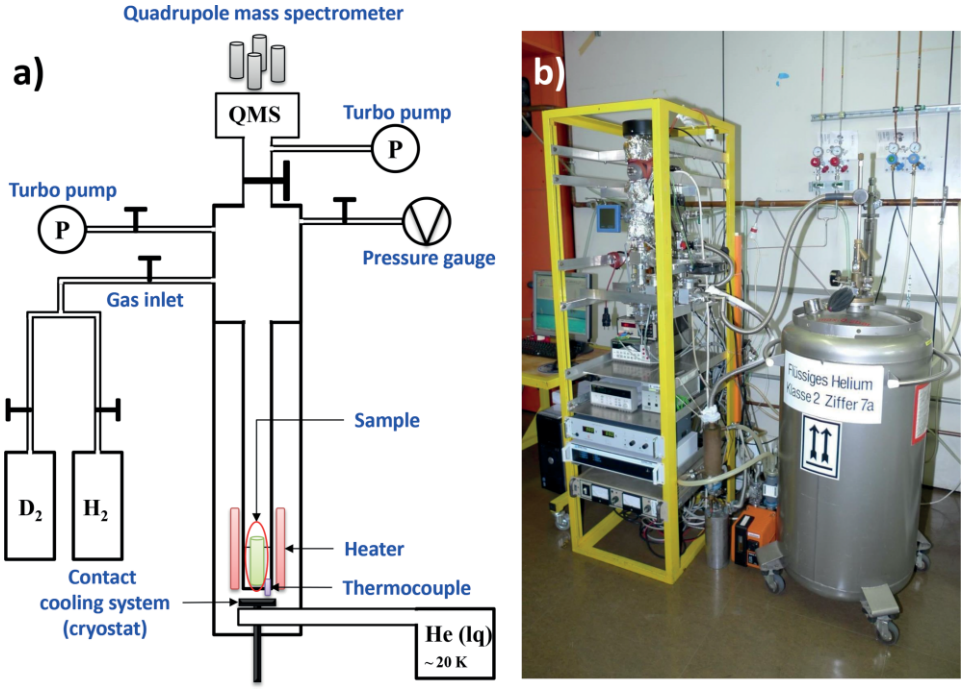

Figure 6. (a) Schematic representation of advanced TDS. (b) Experimental setup for TDS.

preferentially the heavier isotope will be adsorbed at strong binding sites, resulting in separation of isotopes. This is called chemical affinity quantum sieving.

2.3. State-of-the-Art Technique for Direct Measurement of Light Gas Isotope Mixture Selectivity – Advanced Cryogenic Thermal Desorption Spectroscopy (ACTDS)

Up until now, only a few experimental studies based on MOFs have been reported,[9d,15,20] although many promising theoretical and simulation works on quantum sieving have been introduced.[15,19,21] Furthermore, almost all previous experimental studies on D_2/H_2 selectivity have been limited to equilibrium adsorption of pure gas [i.e., $n(D_2)/n(H_2)$ ratio], due to the absence of direct method to measure mixtures, resulting only in estimated selectivity by QS. In order to elucidate the quantum effects, well-designed MOFs have to be investigated with a method that allows direct determination of the selectivity after exposure to an isotope mixture under cryogenic conditions (e.g., at 20–80 K, low pressure).

Thermal desorption spectroscopy (TDS), also known as temperature programmed desorption (TPD), is a standard surface science technique (typical working temperature range of room temp. to 1000 °C), providing information on the binding energies of atomic and molecular species ab/adsorbed on a solid surface. Hirscher's group developed a home-built unique advanced cryogenic thermal desorption spectroscopy apparatus based on this technique (Figure 6); it allows cooling to 20 K and exposure to different isotope gas mixtures.[22] By applying mass spectroscopy the separation factors can be directly determined on gas mixtures, as shown for isotope separation of H_2/D_2 in MOFs.[7b,16]

3. Recent Progress in Hydrogen Isotope Separation Based on MOFs

In 2012 the first and so far only review on quantum sieving with various porous materials was published, concentrating mainly on theoretical work and simulations.[23] The authors discussed the fundamental understanding of factors affecting quantum effects and revealed that equilibrium and kinetic quantum sieving depend strongly on pore size, temperature, and pressure. The results showed that low temperature and a pore size narrower than 0.7 nm were the key factors for quantum effects. Furthermore, because the equilibrium adsorption ratio $n\ D_2/n\ H_2$ was lower than the selectivity achieved through KQS, they concluded that KQS will show encouraging prospects in achieving the separation of hydrogen isotopes. However, they also noted that this field is desperately short of experimental data to confirm the presence of KQS.

In this chapter, we therefore highlight the "experimental results" for hydrogen isotope separation in MOFs or PCPs in order to elucidate the feasibility of quantum sieving. The focus lies on the progress achieved experimentally in understanding the structure–selectivity relationship of H_2/D_2 adsorption in MOFs. Furthermore, two strategies (KQS, CAQS) for technologically relevant mechanisms are introduced.

3.1. Kinetic Quantum Sieving (KQS) in MOFs or PCPs

The first experimental results for the separation of hydrogen and deuterium using MOFs were published in 2008.[20b,24] Chen et al.[20b] were the first, showing that the diffusivity of D_2 was higher than that for H_2 at 77 K in M'MOF-1 (a mixed Zn-MOF possessing a bimodal aperture of 5.6×12 Å^2) and attributed

this to quantum effects (Figure 7, a). However, the difference in D_2 and H_2 diffusivity at 77 K was rather small. In addition, from their virial analysis of the H_2 and D_2 isotherms, D_2–surface interactions slightly stronger than H_2–surface interactions were observed, due to the difference in the quantum statistical mass effect on the vibrational energy levels, whereas D_2–D_2 interactions were weaker than H_2–H_2 interactions because of the higher ZPE of hydrogen (Figure 7, b). They reported that the molar D_2/H_2 ratio at 77 K and 87 K was less than 1.2 and did not change markedly with pressure in the 0.5–100 kPa range (Figure 7, c and d).

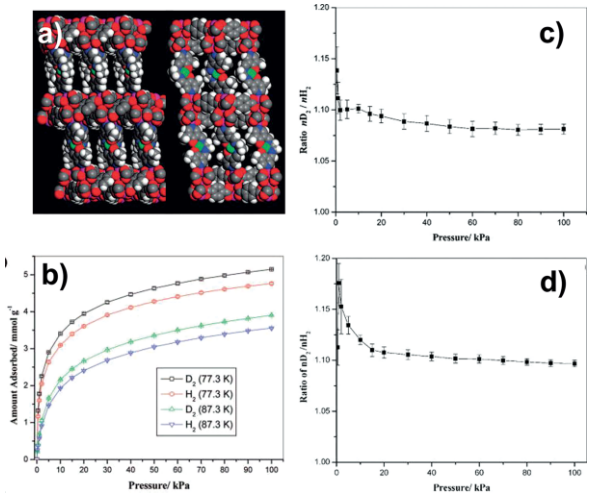

Figure 7. (a) Schematic representation of the frameworks of M'MOF-1. (b) Isotherms for H_2 and D_2 adsorption on M'MOF-1 (pressure range 0–1 bar at 77.3 and 87.3 K). (c) and (d) Variation of $n\,D_2/n\,H_2$ with amount adsorbed for adsorption on M'MOF-1 at 77 K and 87 K. Reprinted from ref.,[20b] with permission. Copyright 2008 American Chemical Society.

Noguchi et al.[24] also measured H_2 and D_2 sorption isotherms on CuBOTf (a Cu-MOF possessing bimodal channels) at 40 K and 77 K and compared the experimental data with theoretical isotherms obtained by quantum-corrected GCMC simulations. The cross-sections of the bi-channels (apertures) of the CuBOTf were 2×2 Å^2 and 8.7×8.7 Å^2 (Figure 8, a). Because the kinetic diameters of the hydrogen isotopes are about 2.83–2.89 Å, [25] they assumed that hydrogen isotope adsorption can only occur in the larger pores. From the measured and simulated pure gas isotherms (Figure 8, b), the selectivity in the case of a 1:1 hydrogen isotope mixture was estimated by applying ideal adsorbed solution theory (IAST[26]) to predict the loading of the gas mixture on MOFs (i.e., assuming no interaction between the adsorbed species and the same chemical potential of an isotope in the gas phase and the adsorbed phase). These calculations yielded the D_2/H_2 molar ratios of 1.2 and 2.6–5.8 (pressure range of 10^{-5} to 10^{-3} MPa) at 77 K and 40 K, respectively (Figure 8, c). However, the selectivity values are semiexperimental results based on assumptions and simplifications.

In a study of carbon molecular sieves (CMSs, Takeda 3A) Bhatia et al. (2010)[18] obtained similar results by quasi-elastic neutron scattering (QENS), showing that D_2 diffuses more rapidly than H_2 below 100 K and that the difference in diffusivity gets stronger on lowering the temperature to 30 K (Figure 9). This

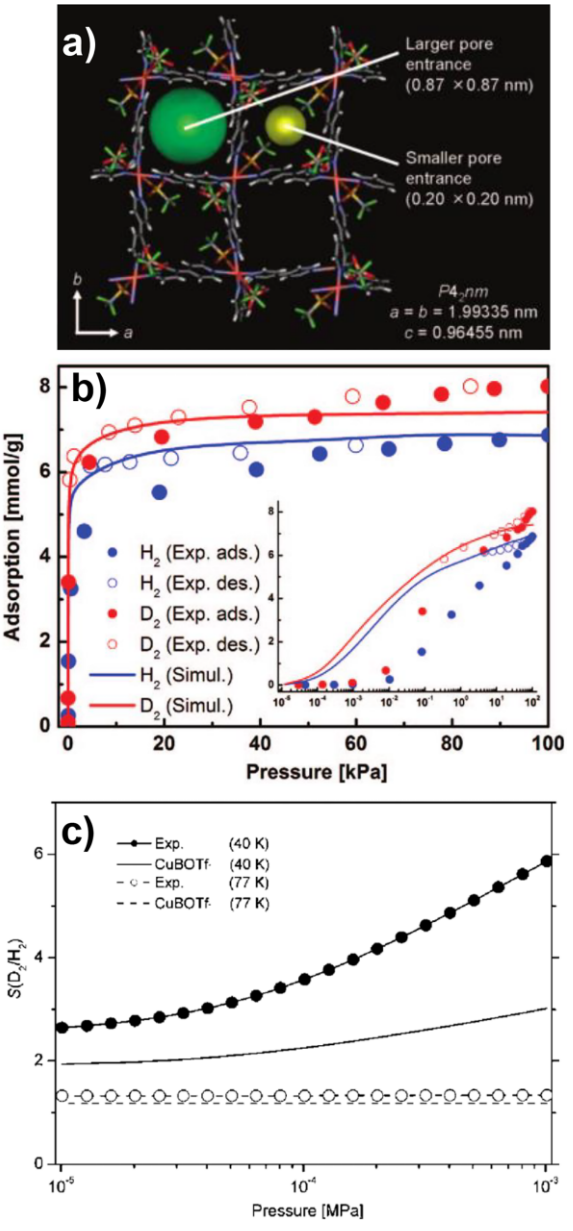

Figure 8. (a) Schematic representation of the frameworks of CuBOTf. (b) Hydrogen and deuterium adsorption isotherms measured at 40 K and simulated by GCMC. (c) The selectivity values at 40 K and 77 K obtained by applying IAST. Reprinted from ref.,[19] with permission. Copyright 2008 American Chemical Society.

QENS result implied that the separation efficiency should be further improvable by exploiting the maximum difference in hydrogen isotope diffusivity.

In quantum sieving, the pore size indeed plays an important role in determining the diffusion kinetics and thereby overall separation. Hence, Oh et al. (2013)[27] investigated a fundamental correlation between isotope separation efficiency and pore diameter (aperture) in four different zeolitic imidazolate frameworks (ZIFs – ZIF-7 and ZIF-8) and COFs (COF-1 and COF-102) with aperture diameters of 3.0 Å, 3.4 Å, 9.0 Å, and 12 Å for ZIF-7, ZIF-8, COF-1, and COF-102, respectively. They observed the tendency to reach a maximum molar ratio ($n\,D_2/n\,H_2$) when

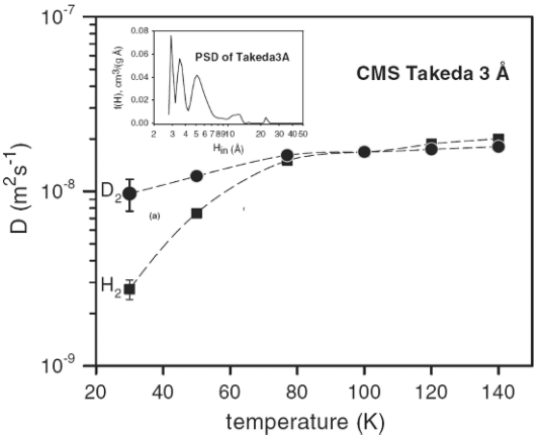

Figure 9. Diffusion coefficients for H_2 and D_2 in Takeda 3 Å CMSs as a function of temperature (loading: 0.5 mmol g^{-1}), showing typical error bars. The inset depicts the pore size distribution of the CMS obtained experimentally from interpretation of observations made at high pressure. Reprinted from ref.,[18] with permission. Copyright 2010 American Physical Society.

the diameter of the aperture was reduced to 3.4 Å (Figure 10). Furthermore, their results suggested that the optimum diameter of the aperture for quantum sieving should lie between 3.0 Å and 3.4 Å. However, a high molar ratio (n D_2/n H_2) was only observed at near zero coverage pressure and low temperature (20 K), which are conditions not suitable for technological application.

3.2. Kinetic Quantum Sieving (KQS) in Temperature-Triggered Flexible MOFs or PCPs

So far, studies of hydrogen isotope separation in most conventional robust porous frameworks have observed high molar ratios only at near zero coverage pressure. In contrast with the robust porous framework, therefore, the soft properties of MOFs or PCPs exhibiting structural flexibility and dynamic properties might be good candidates for enhancing the operating pressure, owing to their unique properties.[28]

Teufel et al. (2013)[7b] assessed the potential of the MFU-4 (metal-organic framework University of Ulm) as a quantum sieve. The framework has a bimodal pore structure with a small A-pore of 3.88 Å and a larger B-pore of 11.94 Å in diameter, with the small and the large pore connected through a narrow aperture of 2.52 Å formed by Cl atoms (Figure 11a and Figure 11, b).[29] Because of this, isotope separation by quantum sieving only works in a very limited size window of the aperture. Usually, the adsorption isotherms indicate decreasing gas uptake with rising adsorption temperature. However, the uptake for hydrogen isotopes in MFU-4 actually increases with increasing sorption temperature. It was found that this interesting adsorption behavior of MFU-4 was attributable to temperature-triggered gate opening due to phonon excitations of Cl atoms at the aperture between the small and large pore (reducing the kinetic diffusion barrier); that is, below the opening temperature gas molecules can barely penetrate, resulting in the enhancement of operating pressure. Furthermore, Teufel et al. presented the first direct measurement of the mixture selectivity by applying a 1:1 D_2/H_2 mixture in an advanced cryogenic thermal desorption spectroscopy (ACTDS) apparatus. Throughout these measurements, the temperature-dependent opening of the aperture in MFU-4(Zn) resulted in a high select-

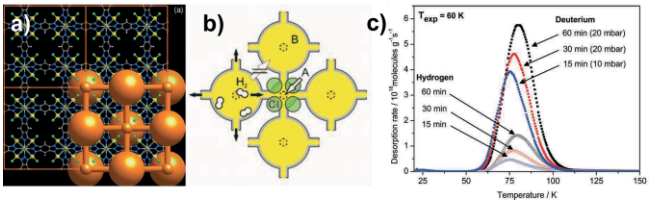

Figure 11. (a) Illustration of the alternating pore structure: the large pore B is only surrounded by small pores A. (b) The A-pore and B-pore are connected by a narrow window (2.52 Å) formed by four chlorine atoms. Any molecule diffusing in the framework has to pass both pores and the connecting window. (c) Hydrogen and deuterium thermal desorption spectra obtained after exposure to a 1:1 mixture at 60 K. Reproduced from ref.,[7b] with permission. Copyright 2013 WILEY-VCH Verlag GmbH.

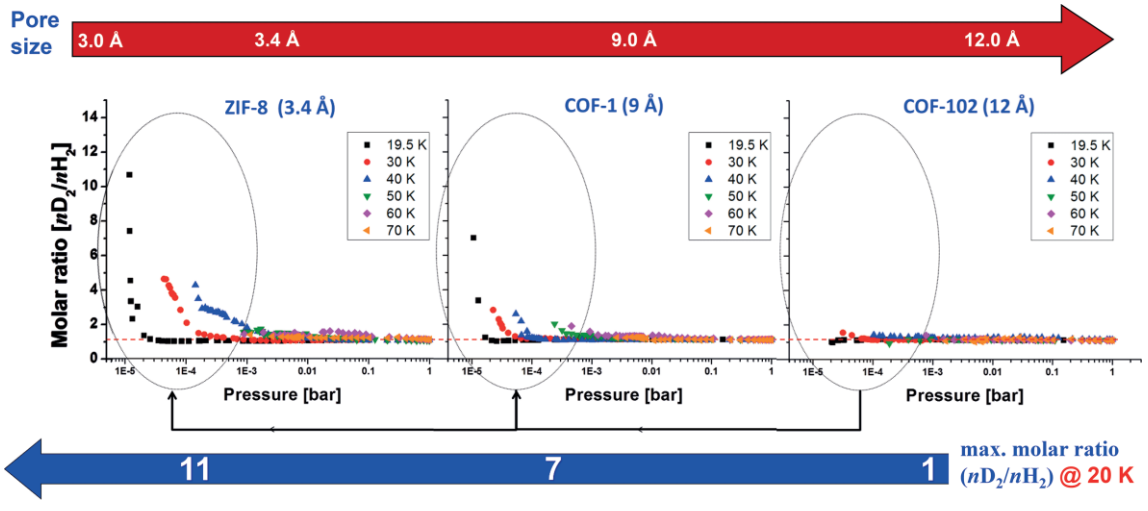

Figure 10. Comparison of the molar D_2/H_2 ratio as function of the effective pore size of organic frameworks over a temperature range of 19.5–70 K and a pressure range of 0–1 bar. Reproduced from ref.,[27] with permission. Copyright 2013 The Royal Society of Chemistry.

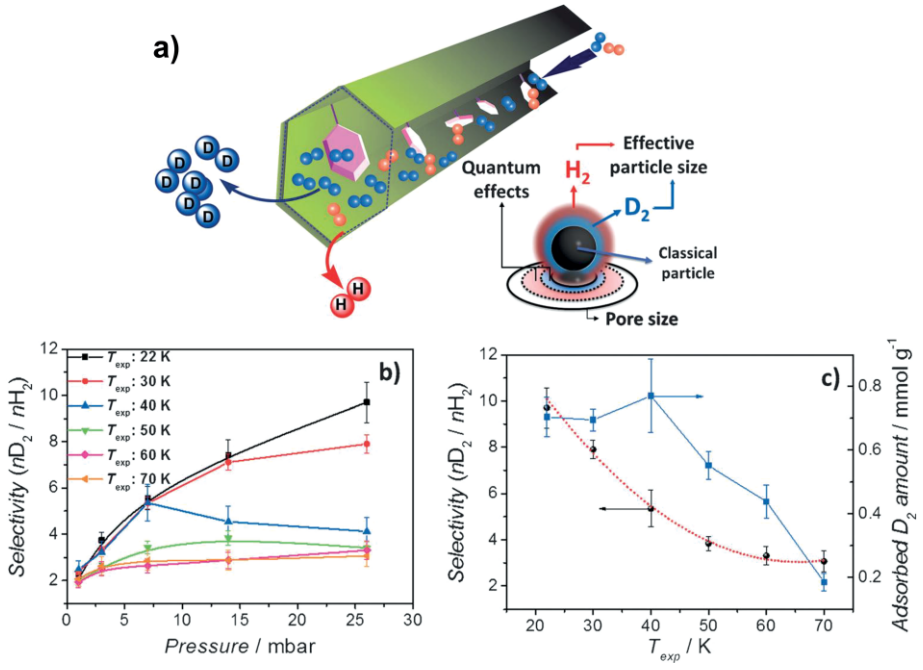

Figure 12. (a) View of the pore channel of COF-1 with dangling pyridine units incorporated in the pore walls. (b) Equimolar mixture selectivity as a function of loading pressure for different temperature. (c) Dependence of the maximum selectivity and corresponding adsorbed D_2 amount. Reproduced from ref.,[7a] with permission. Copyright 2013 WILEY-VCH Verlag GmbH.

ivity of up to 7.5 at 60 K and 10 mbar for short exposure times (15 min).

Oh et al. (2013)[7a] also reported temperature-triggered gate opening in flexible COFs. They successfully synthesized pyridine-decorated COF-1 (Py@COF-1) by a Lewis base approach (Figure 12, a). The Py@COF-1 material has a very densely packed structure with pyridine moieties attached on the pore walls of COF-1, reducing the aperture size and pore volume. Similarly to MFU-4, Py@COF-1 exhibits a varying degree of hysteresis in low-pressure isotherms, indicating changes in the effective aperture size experienced by the adsorbate and thus implying a cryogenically flexible aperture of Py@COF-1.

Oh et al. reported that the selectivity in the case of a 1:1 D_2/H_2 mixture was significantly greater than those of the molar ratios from pure gas isotherms and ascribed this to a quantum isotope effect with cryogenic flexibility. Furthermore, the mixture selectivity increased with pressure and reached its highest value of 9.7 at 26 mbar and 22 K (Figure 12, b and c), greatly superior to the commercial cryogenic distillation process ($S_{D_2/H_2} \approx 1.5$ at 24 K[6]).

Hence, it is evident that the operating pressure can be further enhanced by flexible MOFs and COFs. However, it is interesting to note that their flexibility described here was only a kinetic effect caused by local deformation or vibration (no structural deformation), unlike in typical flexible frameworks in the literature, which are accompanied by a volume change in the framework (e.g., structural deformation of MIL-53).

3.3. Chemical Affinity Quantum Sieving (CAQS) in MOFs with Unsaturated Metal Sites

Despite many experimental investigations on KQS, almost all physisorptive porous frameworks exhibited only rather low isotope separation factors at 77 K (Table 1). As an alternative to kinetic quantum sieving, therefore, hydrogen isotope separation is also possible through exploiting the difference in the zero-point energies of the adsorbed isotopes. Because the different molecular masses of isotopes imply different ZPEs and thereby different adsorption enthalpies (ΔH), this significant ΔH could result in appreciable selectivity even at liquid nitrogen temperature (77 K) and above. In this regard, MOFs are excellent candidates for CAQS because of their versatile functionality (i.e., open metal sites) produced through the incorporation of a high number of unsaturated metal coordination sites in the framework structure.

FitzGerald et al. (2013)[9d] first explored the CAQS behavior in MOFs containing an exceptionally high density of exposed metal cations. They used a family of isostructural MOF-74-M types (M = Fe, Co, Ni),[30] which show the highest adsorption enthalpies for hydrogen recorded for physisorptive porous materials, and measured isotherms over a temperature range of 77–150 K. The isotherms indicate a significantly larger initial heat of adsorption of D_2 over H_2, with the largest difference being 1.4 kJ mol^{-1} (Ni-MOF-74). They applied the ideal adsorption solution theory (IAST) to calculate the selectivity for D_2 over H_2 at 77 K, 87 K, 100 K, 120 K, and 150 K, showing an increase in selectivity from 1.5 at 150 K to 5.0 at 77 K (Figure 13). Furthermore, through infrared measurements on different MOF-74 types, a strong correlation between selectivity and the translational mode frequency of the adsorbed molecule was observed, and from this it was confirmed that the separation is predominant even at high temperature, due to the difference in the zero-point energies of the adsorbed isotopes at these strongly binding sites. Similar work was done by Oh et al. (2014),[7c] who also used CPO-27-Co (also referred to as MOF-

Table 1. Summary of the experimentally reported quantum sieving separability on various MOFs.

Compound	Aperture [Å]	*T* [K]	*P* [mbar]	$R^{[a]}$ (*n* D_2/*n* H_2)	$S^{[b]}$ (1:1 mixture)	Ref.
Porous coordination polymer (CuBOTf)	LPE[c] (8.7*8.7) SPE[d] (0.2*0.2)	40/77	20	5.8/1.2	3.0[f]:1.3[f]	[24]
Microporous mixed MOFs (M'MOF 1)	5.6*12	77/87	< 200	1.15/1.18	–	[20b,21r,25]
12-Connected MOFs	10	77	1000	1.1	–	[31]
HKUST-1	9/5	77	20	1.23	–	[20a]
Coordination frameworks (Cu2L2)	7.3	77	100	1.2	–	[32]
ZIF-7, ZIF-8, COF-1, COF-102,	3,0 3.4, 9.0, 12.0	20	NZP[e]	–, 11, 7, 1	–	[27]
Zn-MFU-4	aperture (2.52) large (11.93) small (3.88)	40/ 50/ 60/ 70	10 / 7–10/ 4–20/ 1.8–10	–/ 4.1/ 2.3/ 1.7	6.9/ 5.8/ 7.5/ 2.8	[7b]
Py@COF-1	2.9	22/ 30/ 40/ 50/ 60/ 70	26/ 26/ 7/ 14/ 26/ 26	–	9.7/ 7.9/ 5.4/ 3.8/ 3.3/ 3.1	[7a]
Ni-MOF-74 Co-MOF-74 Fe-MOF-74	10	77	NZP[e]	4.6/ 3.2/ 2.5	5.0[f]/ 3.2[f]/ 2.5[f]	[9d]
CPO-27(Co)	10	20/ 30/ 40/ 50/ 60/ 70/ 80	30	–	3.0/ 3.7/ 4.5/ 4.5/ 11.8/ 8.4/ 6.3	[7c]

[a] D_2/H_2 molar ratios obtained from the pure gas adsorption isotherms. [b] Experimentally determined (ACTDS) 1:1 D_2/H_2 mixture selectivity. [c] Large pore entrance. [d] Small pore entrance. [e] Near zero coverage pressure. [f] 1:1 D_2/H_2 mixture selectivity from pure gas adsorption isotherms by use of idealized adsorption solution theory (IAST).

74); low-pressure high-resolution adsorption isotherms were measured over the 20–80 K temperature range. Similarly, they observed a strong correlation between selectivity and temperature at these strongly binding sites. In addition, outstanding hydrogen isotope separation at open metal sites was directly

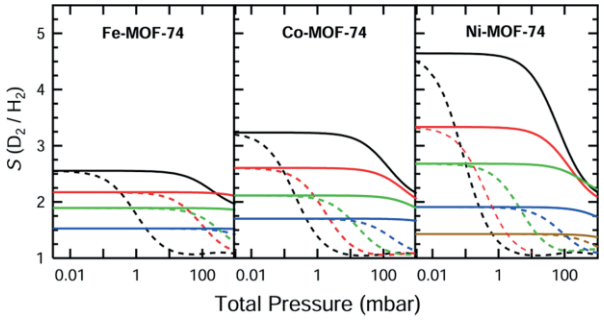

Figure 13. Selectivity (solid curves) for D_2 over H_2 as determined by IAST analysis of the experimentally determined isotherms at 77 K (black), 87 K (red), 100 K (green), 120 K (blue), and 150 K (brown). The dashed curves show the *n* D_2/*n* H_2 ratio at the same temperatures as determined by the two-site Langmuir fit. Reprinted from ref.,[9d] with permission. Copyright 2013 American Chemical Society.

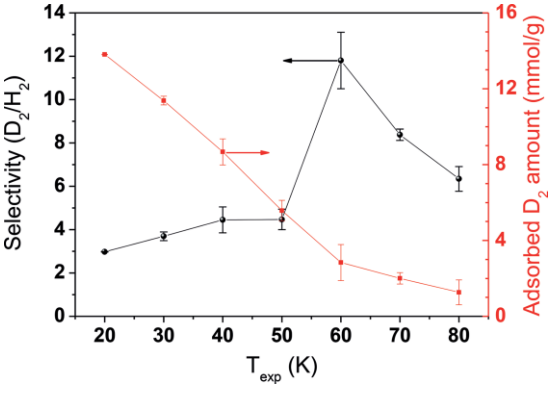

Figure 14. Selectivity in the case of an equimolar hydrogen isotope mixture (30 mbar) as a function of temperature and the corresponding amount of adsorbed D_2. Reproduced from ref.,[7c] with permission. Copyright 2014 American Chemical Society.

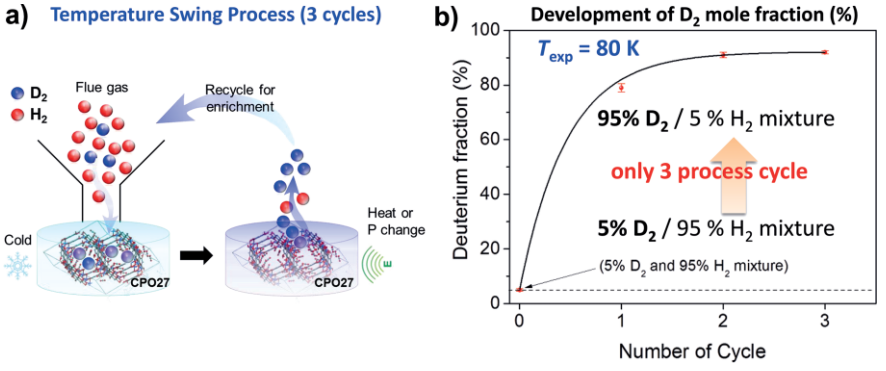

Figure 15. (a) Three-cycle temperature swing process. (b) Development of D_2 mole fraction (%) in a 5 % D_2/95 % H_2 mixture as an initial bulk concentration at 80 K and 30 mbar as function of separation cycle. Reproduced from ref.,[7c] with permission. Copyright 2014 American Chemical Society.

observed through ACTDS. The efficiency of separation of an equimolar D_2/H_2 mixture at 60 K and 30 mbar showed a selectivity of 11.8, the highest so far. Even above liquid nitrogen temperature, the selectivity still exhibited a fairly high value of $S_{D_2/H_2} \approx 6.3$ at 80 K and 30 mbar (Figure 14).

Because the strategy of exploiting open metal sites showed extremely high separation efficiencies even above 77 K, Oh et al. performed three cycles of a temperature swing (range of 80–110 K) deuterium enrichment process that could be directly applied in industrial applications (Figure 15). Remarkably, the results showed that CPO-27-Co enriched very efficiently from isotope mixtures of low (5 %D_2/95 %H_2 isotope mixtures) to high D_2 concentration (95 %D_2/5 %H_2) in only three separation cycles at practical temperatures above 77 K.

In CAQS, most experimental data are basically equilibrium-based measurements, which could exclude the kinetic factor (e.g., diffusion) of H_2 and D_2. Thus, recent research has shown that the strong attraction between the unsaturated metal centers and hydrogen isotopes keeps these sites occupied at relatively high temperature, resulting in high hydrogen isotope separation factors even at temperatures above 77 K. Hence, these results should lead to intelligently designed future porous frameworks for hydrogen isotope separation.

4. Conclusions and Outlook

D_2/H_2 separation is a difficult task because their size, shape, and thermodynamic properties almost mirror each other. In this regard, quantum sieving can be one of the most profitably explored applications of MOFs or PCPs, due to their precisely tunable apertures, their morphologies, and the functionality of the porous frameworks. Hence, this new class of porous frameworks (e.g., MOFs or PCPs) have now opened new avenues for the efficient separation of hydrogen isotopes.

In this microreview we have emphasized and summarized the recent status and future strategies concerning hydrogen isotope separation using porous frameworks (e.g., MOFs or PCPs). Firstly, we described conventional separation techniques (e.g., cryogenic distillation and chemical exchange), which exhibit very high energy costs with low separation efficiencies. Alternatively, two methods based on quantum effects – KQS and CAQS – have been introduced. The correlation between D_2/H_2 molar ratio and the pore size of various MOFs reveals that the molar ratio is strongly dependent on pore size, pressure, and temperature. Higher ratios are reported with smaller pore size and lower *T* and *p*. Furthermore, the results suggest that the pore aperture for quantum sieving should lie between 3.0 and 3.4 Å. Afterwards, two different quantum sieving mechanisms in MOFs and PCPs for isotope separation were introduced. In order to increase the operating pressure, firstly, locally flexible MOFs or PCP have been used for isotope separation, revealing excellent separation efficiency at extremely low temperature (e.g., $S_{D_2/H_2} \approx 10$ at 22 K in Py@COF-1). Although these results show separation factors far superior to those of commercial cryogenic distillation process ($S_{D_2/H_2} \approx 1.5$ at 24 K), it is of greatest interest in industrial application to operate the isotope separation process at higher temperatures (e.g., above liquid nitrogen temperature). In order to fulfil this industrial desire, secondly, the different chemical affinities of isotopes on strong adsorption sites have been utilized in order to allow increases in the operating temperature. The results revealed that MOFs possessing strong binding sites (10–14 kJ mol^{-1} for hydrogen on open metal sites) showed a significantly larger adsorption enthalpy for D_2 over H_2 at the open metal site (ca. 1–2 kJ mol^{-1} difference). Moreover, this strong attraction between the unsaturated metal centers and the hydrogen isotope keeps these sites occupied at relatively high temperatures (even above 77 K). Therefore, strong binding sites lead to large differences in adsorption enthalpy between the isotopes that in turn result in high separation factors at temperatures above 77 K. The highest reported separation efficiency of an equimolar D_2/H_2 mixture in MOFs by CAQS showed a selectivity of 11.8 at 60 K and 30 mbar. Moreover, the selectivity still exhibited a fairly high value of $S_{D_2/H_2} \approx 6.3$ even above liquid nitrogen temperature (80 K and 30 mbar).

Figure 16 shows a summary of all hydrogen isotope separation factors determined for various porous frameworks as a function of working temperature. It clearly reveals that use of MOFs with CAQS shows encouraging prospects with high selectivity at high operating temperatures to achieve efficient separation of hydrogen isotopes. Furthermore, CAQS in MOFs has been experimentally tested by a temperature swing process, revealing that deuterium can be easily enriched within a temperature window of 80 to 110 K. These results demonstrate

the high potential of MOFs for application in hydrogen isotope separation.

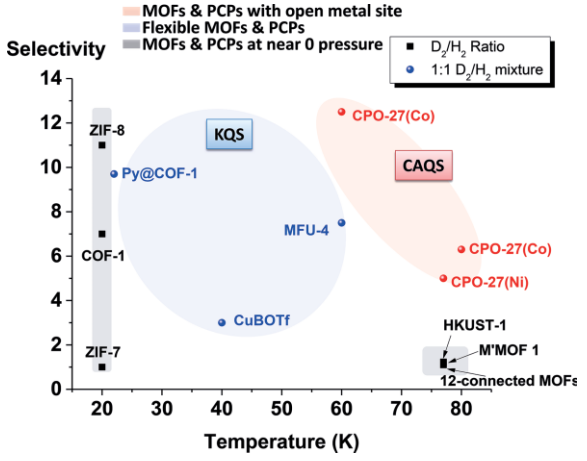

Figure 16. Hydrogen isotope separation factors for various porous frameworks as a function of working temperature.

Hence, future challenges will evidently be related to using the information garnered from the study of both KQS and CAQS in the isotope separation field in order to design new and effective porous frameworks. In particular, porous materials exhibiting both effects (KQS and CAQS) would be beneficial for very effective hydrogen isotope separation. For example, an intelligently designed porous material could be a core-shell MOF possessing sufficiently flexible apertures (outer part) and numerous open metal sites (inner part). Hence, a flexible aperture would enhance the D_2 uptake relative to H_2, resulting in an enriched deuterium concentration inside the MOF. Then, strong binding sites would selectively capture the deuterium, leading to enhanced selectivity.

Although at the current level of development many practical challenges still remain to be solved, quantum sieving by MOFs will, in our opinion, soon be a very efficient and effective way to separate hydrogen isotopes.

Acknowledgments

This research was supported by the National R&D Program (NRF-2016M1A7A1A02005285) and the Basic Science Research Program (NRF-2016R1C1B1007364) through the National Research Foundation of Korea (NRF) funded by the Ministry of Science, ICT and Future Planning.

Keywords: Isotopes · Hydrogen · Deuterium · Isotope separation · Metal organic frameworks · Quantum sieving · Quantum chemical affinity sieving

[1] a) M. I. Hoffert, K. Caldeira, G. Benford, D. R. Criswell, C. Green, H. Herzog, A. K. Jain, H. S. Kheshgi, K. S. Lackner, J. S. Lewis, H. D. Lightfoot, W. Manheimer, J. C. Mankins, M. E. Mauel, L. J. Perkins, M. E. Schlesinger, T. Volk, T. M. L. Wigley, *Science* **2002**, *298*, 981–987; b) K. Tokimatsu, J. i. Fujino, S. Konishi, Y. Ogawa, K. Yamaji, *Energy Policy* **2003**, *31*, 775–797; c) R. E. Smalley, *Mrs Bull.* **2005**, *30*, 412–417; d) N. Armaroli, V. Balzani, *Angew. Chem. Int. Ed.* **2007**, *46*, 52–66; *Angew. Chem.* **2007**, *119*, 52.

[2] S. P. I. Pázsit, *Nucl. Sci. Eng.* **2006**, *154*, 367–373.

[3] P. P. Povinec, H. Bokuniewicz, W. C. Burnett, J. Cable, M. Charette, J. F. Comanducci, E. A. Kontar, W. S. Moore, J. A. Oberdorfer, J. de Oliveira, R. Peterson, T. Stieglitz, M. Taniguchi, *J. Environ. Radioact.* **2008**, *99*, 1596–1610.

[4] J. Daillant, *Lecture Notes in Physics* **2016**, *917*, 413–444.

[5] N. N. Greenwood, A. Earnshaw, *Chemistry of the Elements (2nd ed.)*, Butterworth-Heinemann, Oxford, UK, **1997**.

[6] H. K. Rae, in: *Separation of Hydrogen Isotopes*, vol. 68, American Chemical Society, **1978**, p. 1–26.

[7] a) H. Oh, S. B. Kalidindi, Y. Um, S. Bureekaew, R. Schmid, R. A. Fischer, M. Hirscher, *Angew. Chem. Int. Ed.* **2013**, *52*, 13219–13222; *Angew. Chem.* **2013**, *125*, 13461; b) J. Teufel, H. Oh, M. Hirscher, M. Wahiduzzaman, L. Zhechkov, A. Kuc, T. Heine, D. Denysenko, D. Volkmer, *Adv. Mater.* **2013**, *25*, 635–639; c) H. Oh, I. Savchenko, A. Mavrandonakis, T. Heine, M. Hirscher, *ACS Nano* **2014**, *8*, 761–770.

[8] J. J. M. Beenakker, V. D. Borman, S. Y. Krylov, *Chem. Phys. Lett.* **1995**, *232*, 379–382.

[9] a) H. Kagita, T. Ohba, T. Fujimori, H. Tanaka, K. Hata, S.-i. Taira, H. Kanoh, D. Minami, Y. Hattori, T. Itoh, H. Masu, M. Endo, K. Kaneko, *J. Phys. Chem. C* **2012**, *116*, 20918–20922; b) S. Niimura, T. Fujimori, D. Minami, Y. Hattori, L. Abrams, D. Corbin, K. Hata, K. Kaneko, *J. Am. Chem. Soc.* **2012**, *134*, 18483–18486; c) C. Pierce, Oberlin College, USA, **2012**; d) S. A. FitzGerald, C. J. Pierce, J. L. C. Rowsell, E. D. Bloch, J. A. Mason, *J. Am. Chem. Soc.* **2013**, *135*, 9458–9464.

[10] V. Dingenen, A. W. van Itterbeek, *Physica* **1939**, *6*, 49–58.

[11] R. Yaris, J. R. Sams, *J. Chem. Phys.* **1962**, *37*, 571–576.

[12] F. Stéphanie-Victoire, A.-M. Goulay, E. Cohen de Lara, *Langmuir* **1998**, *14*, 7255–7259.

[13] X. B. Zhao, S. Villar-Rodil, A. J. Fletcher, K. M. Thomas, *J. Phys. Chem. B* **2006**, *110*, 9947–9955.

[14] D. Noguchi, Y. Hattori, C. M. Yang, Y. Tao, T. Konishi, T. Fujikawa, T. Ohkubo, Y. Nobuhara, T. Ohba, H. Tanaka, H. Kanoh, M. Yudasaka, S. Iijima, H. Sakai, M. Abe, Y. J. Kim, M. Endo, K. Kaneko, in: *ECS Transactions*, vol. 11, 8th ed. **2007**, p. 63–75.

[15] H. Tanaka, D. Noguchi, A. Yuzawa, T. Kodaira, H. Kanoh, K. Kaneko, *J. Low Temp. Phys.* **2009**, *157*, 352–373.

[16] I. Krkljus, T. Steriotis, G. Charalambopoulou, A. Gotzias, M. Hirscher, *Carbon* **2013**, *57*, 239–247.

[17] P. Kowalczyk, P. A. Gauden, A. P. Terzyk, S. Furmaniak, *J. Phys. Condens. Matter* **2009**, *21*, 144210.

[18] T. X. Nguyen, H. Jobic, S. K. Bhatia, *Phys. Rev. Lett.* **2010**, *105*, 085901.

[19] Y. Jiao, A. Du, M. Hankel, S. C. Smith, *Phys. Chem. Chem. Phys.* **2013**, *15*, 4832–4843.

[20] a) K. M. Thomas, B. Xiao, P. S. Wheatley, X. B. Zhao, A. J. Fletcher, S. Fox, A. G. Rossi, I. L. Megson, S. Bordiga, L. Regli, R. E. Morris, *J. Am. Chem. Soc.* **2007**, *129*, 1203–1209; b) B. Chen, X. Zhao, A. Putkham, K. Hong, E. B. Lobkovsky, E. J. Hurtado, A. J. Fletcher, K. M. Thomas, *J. Am. Chem. Soc.* **2008**, *130*, 6411–6423; c) K. M. Thomas, *Dalton Trans.* **2009**, 1487–1505.

[21] a) H. Tanaka, J. Fan, H. Kanoh, M. Yudasaka, S. Iijima, K. Kaneko, *Mol. Simul.* **2005**, *31*, 465–474; b) H. Tanaka, H. Kanoh, M. Yudasaka, S. Lijima, K. Kaneko, *J. Am. Chem. Soc.* **2005**, *127*, 7511–7516; c) S. K. Bhatia, A. L. Myers, *Langmuir* **2006**, *22*, 1688–1700; d) X.-Z. Chu, Y.-P. Zhou, Y.-Z. Zhang, W. Su, Y. Sun, L. Zhou, *J. Phys. Chem. B* **2006**, *110*, 22596–22600; e) G. Garberoglio, M. M. DeKlavon, J. K. Johnson, *J. Phys. Chem. B* **2006**, *110*, 1733–1741; f) Y. Hattori, H. Tanaka, F. Okino, H. Touhara, Y. Nakahigashi, S. Utsumi, H. Kanoh, K. Kaneko, *J. Phys. Chem. B* **2006**, *110*, 9764–9767; g) A. V. A. Kumar, S. K. Bhatia, ***2006** International Conference on Nanoscience and Nanotechnology*, vol. 1 and 2, **2006**, 459–462; h) T. Lu, E. M. Goldfield, S. K. Gray, *J. Phys. Chem. B* **2006**, *110*, 1742–1751; i) P. Kowalczyk, P. A. Gauden, A. P. Terzyk, S. K. Bhatia, *Langmuir* **2007**, *23*, 3666–3672; j) A. V. A. Kumar, H. Jobic, S. K. Bhatia, *Adsorption* **2007**, *13*, 501–508; k) P. Kowalczyk, P. A. Gauden, A. P. Terzyk, *J. Phys. Chem. B* **2008**, *112*, 8275–8284; l) A. V. A. Kumar, S. K. Bhatia, *J. Phys. Chem. C* **2008**, *112*, 11421–11426; m) X. Z. Chu, Y. J. Zhao, Y. H. Kan, W. G. Zhang, S. Y. Zhou, Y. P. Zhou, L. Zhou, *Chem. Eng. J.* **2009**, *152*, 428–433; n) G. Garberoglio, *Chem. Phys. Lett.* **2009**, *467*, 270–275; o) S. Utsumi, M. Arai, M. Kanamaru, K. Urita, T. Fujimori, N. Yoshizawa, D. Noguchi, K. Nishiyama, Y. Hattori, F. Okino, T. Ohba, H. Tanaka, H. Kanoh, K. Kaneko, *Nano Lett.* **2009**, *9*, 3694–3698; p) Y. Wang, S. K. Bhatia, *J. Phys. Chem. C* **2009**,

113, 14953–14962; q) B. K. Carpenter, *Nat. Chem.* **2010**, *2*, 80–82; r) B. L. Chen, S. C. Xiang, G. D. Qian, *Acc. Chem. Res.* **2010**, *43*, 1115–1124; s) G. Garberoglio, J. K. Johnson, *ACS Nano* **2010**, *4*, 1703–1715; t) F. Furtado, P. Galvosas, M. Goncalves, F. D. Kopinke, S. Naumov, F. Rodriguez-Reinoso, U. Roland, R. Valiullin, J. Karger, *J. Am. Chem. Soc.* **2011**, *133*, 2437–2443; u) D. Liu, W. Wang, J. Mi, C. Zhong, Q. Yang, D. Wu, *Ind. Eng. Chem. Res.* **2011**, *51*, 434–442; v) H. Tanaka, M. T. Miyahara, *J. Chem. Eng. Jpn.* **2011**, *44*, 355–363; w) A. Gotzias, T. Steriotis, *Mol. Phys.* **2012**, *110*, 1179–1187; x) G. C. A. Gotzias, A. Ampoumogli, I. Krkljus, M. Hirscher, Th. Steriotis, *Adsorption* **2013**, *19*, 373–379.

[22] a) B. Panella, M. Hirscher, B. Ludescher, *Microporous Mesoporous Mater.* **2007**, *103*, 230–234; b) B. Panella, K. Hones, U. Muller, N. Trukhan, M. Schubert, H. Putter, M. Hirscher, *Angew. Chem. Int. Ed.* **2008**, *47*, 2138–2142; *Angew. Chem.* **2008**, *120*, 2169.

[23] J. Cai, Y. Xing, X. Zhao, *RSC Adv.* **2012**, *2*, 8579–8586.

[24] D. Noguchi, H. Tanaka, A. Kondo, H. Kajiro, H. Noguchi, T. Ohba, H. Kanoh, K. Kaneko, *J. Am. Chem. Soc.* **2008**, *130*, 6367–6372.

[25] J.-R. Li, R. J. Kuppler, H.-C. Zhou, *Chem. Soc. Rev.* **2009**, *38*, 1477–1504.

[26] N. F. Cessford, N. A. Seaton, T. Düren, *Ind. Eng. Chem. Res.* **2012**, *51*, 4911–4921.

[27] H. Oh, K. S. Park, S. B. Kalidindi, R. A. Fischer, M. Hirscher, *J. Mater. Chem. A* **2013**, *1*, 3244–3248.

[28] a) A. J. Fletcher, K. M. Thomas, M. J. Rosseinsky, *J. Solid State Chem.* **2005**, *178*, 2491–2510; b) S. Kitagawa, K. Uemura, *Chem. Soc. Rev.* **2005**, *34*, 109–119; c) S. Horike, S. Shimomura, S. Kitagawa, *Nat. Chem.* **2009**, *1*, 695–704; d) Z.-J. Lin, J. Lu, M. Hong, R. Cao, *Chem. Soc. Rev.* **2014**, *43*, 5867–5895.

[29] D. Denysenko, M. Grzywa, M. Tonigold, B. Streppel, I. Krkljus, M. Hirscher, E. Mugnaioli, U. Kolb, J. Hanss, D. Volkmer, *Chem. Eur. J.* **2011**, *17*, 1837–1848.

[30] M. T. Kapelewski, S. J. Geier, M. R. Hudson, D. Stück, J. A. Mason, J. N. Nelson, D. J. Xiao, Z. Hulvey, E. Gilmour, S. A. FitzGerald, M. Head-Gordon, C. M. Brown, J. R. Long, *J. Am. Chem. Soc.* **2014**, *136*, 12119–12129.

[31] J. Jia, X. Lin, C. Wilson, A. J. Blake, N. R. Champness, P. Hubberstey, G. Walker, E. J. Cussen, M. Schroder, *Chem. Commun.* **2007**, 840–842.

[32] X. Lin, J. Jia, X. Zhao, K. M. Thomas, A. J. Blake, G. S. Walker, N. R. Champness, P. Hubberstey, M. Schröder, *Angew. Chem. Int. Ed.* **2006**, *45*, 7358–7364; *Angew. Chem.* **2006**, *118*, 7518.

Received: March 7, 2016
Published Online: June 22, 2016